

Principles Governing the Binding of a Class of Non-Peptidic Inhibitors to the SH2 Domain of src Studied by X-ray Analysis

Guadrin Lange,^{†,‡} Dominique Lesuisse,^{*,§} Pierre Deprez, Bernard Schoot, Petra Loenze, Didier Bénard, Jean-Pierre Marquette, Pierre Broto, Edoardo Sarubbi, and Eliane Mandine

Aventis Pharma, 102 Route de Noisy, 93235 Romainville, France

Received October 29, 2001

A total of 11 structures of the pp60src SH2 domain with non-peptidic inhibitors based on the same two closely related inhibitor scaffolds were determined using X-ray crystallography. Surprisingly, the inhibitors that have an IC₅₀ value between 4 and 2700 nM bind in three different binding modes. Structure comparisons show that the inhibitors aim to maximize the interaction between the hydrophobic substituent and the hydrophobic pY+3 pocket. This is achieved either by an alternative binding mode of the phenyl phosphate or by including water molecules that mediate the interaction between the inhibitor scaffold and a rigid surface of the SH2 domain. The combination of the rigid pY+3 pocket and the rigid protein surface to which the scaffolds bind results in severe distance and angular restraints for putative scaffolds and their substituents. The X-ray data suggest that these restraints seem to be compensated in our system by including water molecules, thereby increasing the flexibility of the system.

Introduction

pp60src kinase is a multidomain protein that plays a role in signal transduction.¹ It has been implicated in osteoclast-mediated bone resorption and thus represents a therapeutic target for the treatment of osteoporosis and other bone-related diseases.^{2,3} Of particular interest are inhibitors binding to the SH2 domain of pp60src kinase. SH2 domains are common protein recognition motifs that have a highly conserved sequence and 3D structure and bind preferentially phosphotyrosine(pY)-containing peptides.⁴ A considerable number of crystal structures of different SH2 domains with peptides and also non-peptidic inhibitors have been described.^{5–10} With few exceptions,^{11,12} the peptidic and non-peptidic ligands bind in an extended conformation resembling a two-pronged plug. A flat protein surface is located between the two major interaction sites, i.e., the hydrophilic phosphotyrosine binding pocket and the hydrophobic pY+3 pocket. Hence, most of the corresponding inhibitors can be described as scaffolds that interact with the flat surface and two substituents pointing into the phosphotyrosine and the pY+3 pocket.

Structure-based drug design is usually based on a limited number of experimentally obtained protein–ligand complexes only. The binding affinity of related compounds is subsequently predicted using molecular modeling tools. However, sometimes there are difficulties in correlating the predicted binding affinities with their corresponding experimental values. In cases for which subsequently an experimental 3D structure was obtained, it turned out that these discrepancies were

very often due to different binding modes of the inhibitor.^{13,14} Thus, to predict binding affinities successfully, it is essential to understand the driving force of inhibitor binding and in particular the principles according to which a certain binding mode is assumed. Experimentally determined 3D structures reveal the details of inhibitor binding at the atomic level. In addition, by examination of the superposition of a variety of closely related inhibitor complex structures, the importance of specific interactions and the principles governing the inhibitor binding become visible.

Here, we present experimental evidence that the same non-peptidic scaffold binds to the SH2 domain of pp60src with different binding modes. The individual binding modes differ in the number of water molecules that mediate the interaction between the scaffold and the SH2 domain. Eleven X-ray structures with inhibitors that have two different but closely related scaffolds were determined at high resolution. On the basis of the comparison of their X-ray structures, the driving force for inhibitor binding and the reason that a certain binding mode is present will be analyzed. In particular, the role of the mediating water molecules will be investigated.

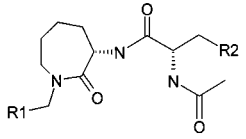
Materials and Methods

Human pp60src SH2 crystals were grown at 4 °C using a dialysis approach. Protein (60–80 mg/mL in citrate buffer at pH 5.5, 10 mM DTT) was dialyzed against an aqueous solution of 10 mM DTT.¹⁵ After one night, cubic-shaped single crystals are observed. The crystals were soaked overnight with the corresponding inhibitor solution (Table 1) and prior to data collection with 10% of glycerol as cryoprotectant.¹⁶ Data were collected at –170 °C on a Mar345 imaging system mounted on a rotating anode X-ray generator (GX21, Enraf Nonius). The data were processed using XDS¹⁷ and refined using X-PLOR¹⁸ based on a model provided by Ariad.¹⁵ Model building and structure comparison were carried out using Quanta.¹⁹ Prior to their comparison, all structures were superimposed using LSQKAB.²⁰ The most important details

* To whom correspondence should be addressed. Phone: +33-1-48933771. Fax: +33-1-58932466. E-mail: dominique.lesuisse@aventis.com.

[†] Aventis Pharma, Structural Biology, 65926 Frankfurt, Germany.
[‡] Present address: Aventis Crop Science, Hit Discovery, 65926 Frankfurt, Germany.

[§] Present address: Aventis Research Centre, 13 Quai Jules Guesde, 94403 Vitry, France.

Table 1. Nonpeptidic Inhibitors of SH2 Domain of src


Compound	IC ₅₀ [nM]	R1	R2
Compound 1	5		
Compound 2	9		
Compound 3	290		
Compound 5	340		
Compound 6	143		
Compound 8	3		
Compound 9	450		
Compound 10	0.25		
Compound 11	2000		

Compound	IC ₅₀ [nM]	R1	R2
Compound 4	2700	S	
Compound 7	2300	C	

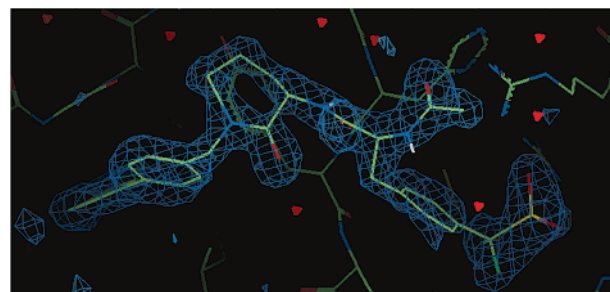
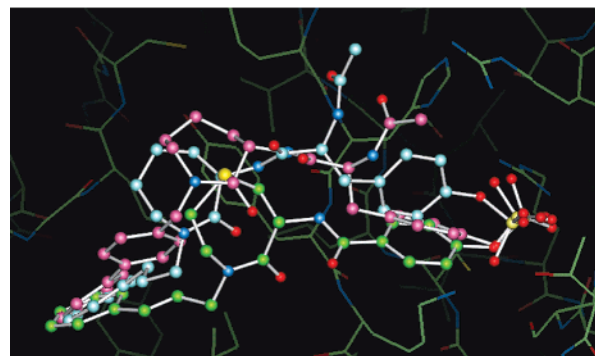
of the data collection and structure refinement are summarized in Table 2. The IC₅₀ values were measured as described earlier.¹⁶ The compounds were synthesized as described in refs 16, 22, and 23.

Results

A total of eleven X-ray structures of SH2 complexes with inhibitors containing two closely related seven-membered ring scaffolds (Table 1) have been determined. Scaffold II differs from scaffold I by an insertion of an acetamidomethylene moiety. The inhibitors were non-peptidic and had IC₅₀ values ranging from 4 to 2700 nM. The quality of the X-ray structures was in all cases excellent, with most of the crystals diffracting beyond 0.2 nm. A typical omit map displaying the electron density of compound **1** is presented in Figure 1. A

Table 2. X-ray Data for Complexes of the SH2 Domain with Compounds **1–11**

compound	resolution [nm]	R _{merge} [%]	R _{factor} [%]
1	0.180	7.7	19.2
2	0.170	6.8	19.2
3	0.195	7.9	18.4
4	0.180	7.8	20.0
5	0.210	9.1	17.9
6	0.170	4.9	19.6
7	0.180	5.7	20.8
8	0.195	5.4	19.4
9	0.165	6.6	20.7
10	0.180	7.7	20.0
11	0.185	5.0	19.6
citrate	0.155	4.8	19.1

**Figure 1.** Omit map of compound **1** bound to the SH2 domain of src.**Figure 2.** Superposition of compounds **2** (pink), **3** (blue), and **4** (green) bound to the SH2 domain of src.

superposition of these structures shows that there are different binding modes present even though the inhibitors are closely related. In particular, the binding modes of the inhibitor scaffolds differ significantly between individual compounds, resulting in a considerably different localization of the inhibitor within the binding region. A closer inspection revealed that there are three main binding modes that may be represented by compounds **2–4** (Figure 2).

Inhibitor Binding Mode of Compound 2. The interaction of compound **2** (IC₅₀ = 9 nM) with the SH2 domain of src is shown in Figure 3a. The phosphate group forms salt bridges to the arginine side chains of R14 and R34 and H bonds to the amide nitrogen of E37 and the side chain of T38 (not shown). Additional H bonds are formed between an amide nitrogen of compound **2** and the carbonyl oxygen of H60 and between the carbonyl oxygen of the acetamido moiety of compound **2** and the side chain of R14. Further stabilization is derived from two water molecules that link the acetamido moiety to H60N and the lactam carbonyl group to K62N via hydrogen bonds. Major hydrophobic interactions exist between the biphenyl moiety and

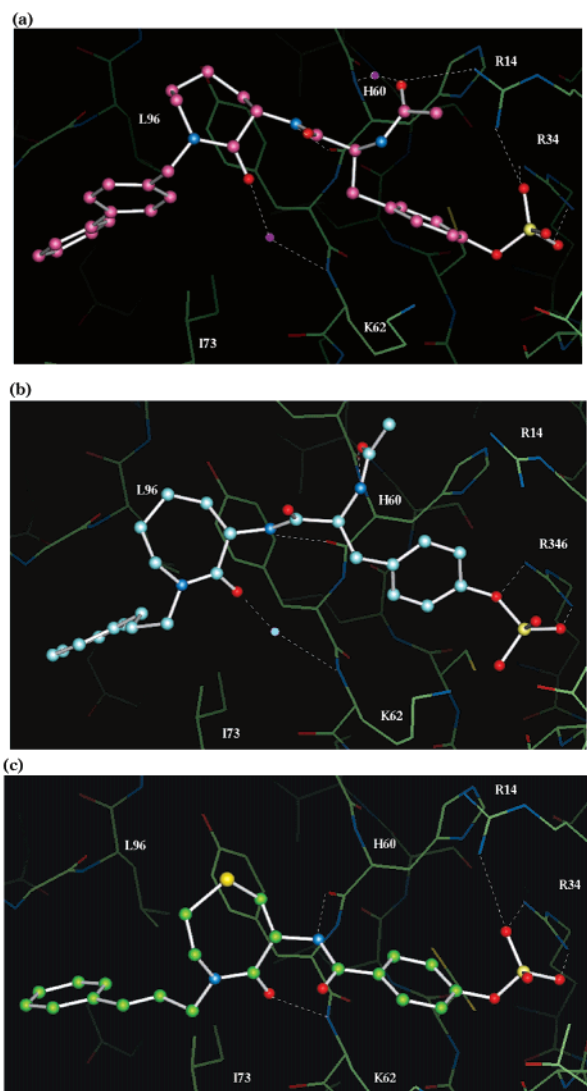


Figure 3. (a) Interaction of compound **2** with the SH2 domain of src. (b) Interaction of compound **3** with the SH2 domain of src. (c) Interaction of compound **4** with the SH2 domain of src.

protein residues 94–96 and 73–74. A second, minor hydrophobic interaction is found between the caprolactam scaffold itself and Y61.

The superposition of compound **2** with the pYEEI peptide^{5,24} shows that both compounds display the same binding mode. The interaction of the phosphotyrosine and the acetamido moiety with the protein is identical. In addition, the conformation and the interaction of the backbone of the pYEEI peptide and the inhibitor scaffold with the SH2 domain are very similar, including all H bonds made to the protein or to water molecules bridging to the protein. Both glutamate side chains of the pYEEI peptide point toward the solvent. The side chain of the isoleucine points into the pY+3 pocket. The main-chain atoms, including the carboxy terminus of the peptide, have no significant interaction with the protein. The side chain of the first glutamate is replaced in compound **2** by a lactam ring that interacts favorably with Y61. Compared to the isoleucine side chain in the pYEEI peptide, the biphenyl moiety in compound **2** fits better in the hydrophobic pocket, resulting in a total of 15 carbon–carbon distances shorter than 0.4 nm compared to 6 distances for the corresponding isoleucine side chain in the pYEEI peptide.

Inhibitor Binding Mode of Compound 3. The interaction of the phosphate group in compound **3** ($IC_{50} = 290$ nM) with the side chains of R14 and R34 is different compared to that in compound **2** (Figure 3b). In this structure, the salt bridges are not formed by two terminal oxygens such as in compound **2** but one terminal oxygen and the ester oxygen of the phosphate ester. This results in an alternative conformation of the phosphotyrosine ring, which is accompanied by a novel interaction of the acetamido moiety with the protein. The acetamido moiety of compound **3** interacts with the H60N, and one amide nitrogen of compound **3** forms an H bond to H60O. The interaction of the lactam carbonyl oxygen to K62N is bridged by a water molecule. The lactam ring, including the phenyl ring, is shifted compared to that in compound **2** in a way that the terminal benzyl ring is now positioned comfortably in the hydrophobic pocket. The conformation of the phenyl phosphate moiety found in compound **3** corresponds to the conformation found in the complex structure with phenyl phosphate.²¹

Inhibitor Binding Mode of Compound 4. The interaction of compound **4** with the hydrophobic pY+3 pocket and the phosphotyrosine binding site is very similar to that found in compound **2** even though compound **4** ($IC_{50} = 2700$ nM) is shortened by two carbon atoms compared to compound **2** (Figure 3d) to achieve the inhibitor adopting an alternative binding mode of the scaffold. There are no water molecules bridging compound **4** and the protein. Instead, H bonds are formed between the amide nitrogen of the inhibitor to H60O and the lactam carbonyl of compound **4** to K62N. As a result, the terminal ring is comfortably positioned in the hydrophobic pocket, resulting in a total of 11 carbon–carbon distances between the inhibitor and the protein shorter than 0.4 nm.

Characterization of the Scaffold Binding Mode.

An analysis of the superimposed structures suggests that the binding modes of the scaffolds can be characterized on the basis of the H-bond pattern formed between the individual scaffold and the protein. SH2 has three main-chain H-bond donors/acceptors that need to be satisfied: H60N, H60O, and K62N. They belong to a rigid surface of the protein, as judged from the low-temperature factors and the very limited rms deviations between individual X-ray structures. In addition, the side chain of R14 is available for hydrogen bonding. In all structures, these H-bond partners are satisfied by interacting directly with the inhibitor scaffold or the interaction is mediated by a water molecule. When a water molecule mediates the inhibitor–protein interaction, the water molecule is exactly at the position in which the H-bond partner within the inhibitor scaffold is otherwise located (Figure 4a). The individual binding modes represented by compounds **2–4** differ in the details of their H-bond pattern formed between the inhibitor scaffold and the SH2 domain of src (Figure 4b). While the scaffold in compound **4** interacts in all cases directly with the protein backbone, the interaction of the scaffold of compound **3** with the protein backbone includes one bridging water molecule and the scaffold of compound **2** includes two bridging water molecules.

The relative position of the individual H-bond partners within the inhibitor are crucial in order to satisfy

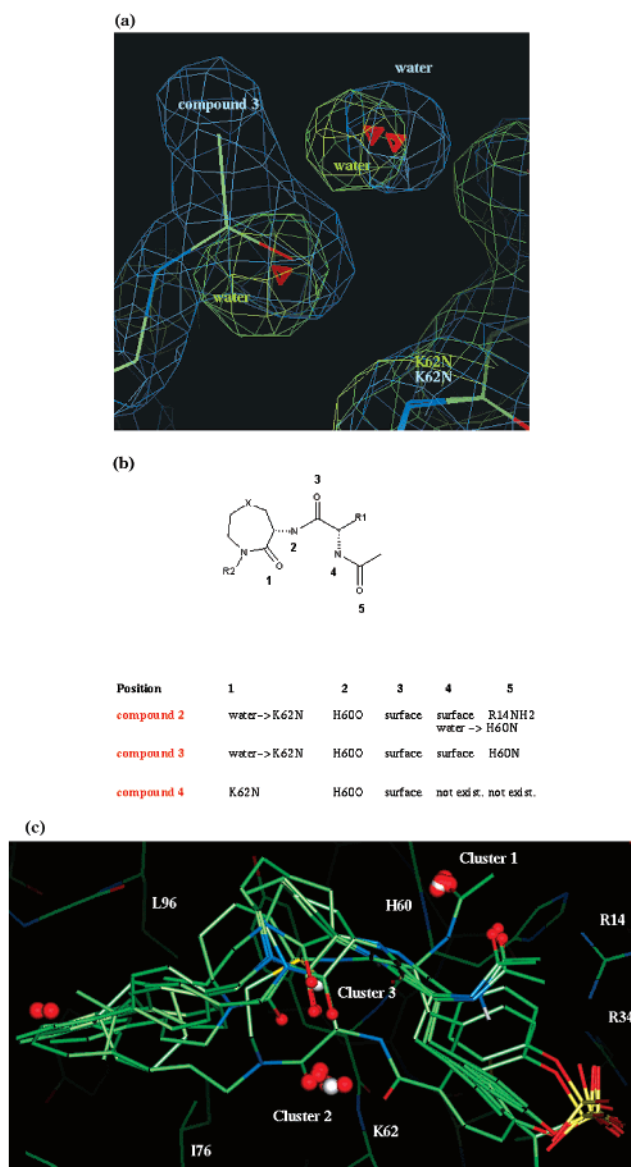


Figure 4. (a) Superposition of the electron density of compounds **3** (green) and **4** (blue). (b) Characterization of the H-bond patterns in the SH2 complexes. (c) Localization of the position of H-bond acceptors including water molecules in the structure of compounds **2–7**. In addition, the positions of the water molecules in the citrate structure are indicated in white.

the constraints that the H bonds to H60N, H60O, and K62N have to be made. This can be visualized by superimposing X-ray structures that differ in their pY+3 substituent or assume different binding modes. Figure 4c shows the positions of H-bond acceptors in compounds **2–7**, including the water molecules that mediate the interaction between the protein and some of the inhibitors. The positions of these H-bond acceptors form two well-defined clusters for the H-bond acceptors interacting directly with the protein. In structures with small ligands such as citrate, there are well-defined water molecules located at these positions, highlighting the importance of an H-bond acceptor present at these positions. Because of the angular and distance restraints of H bonds and the rigidity of the protein surface, clusters 1 and 2 are limited in their size (Figure 4c). However, the positions of the second-layer H-bond acceptors are much less restrained and cluster 3, which

is formed by second-layer inhibitor H-bond acceptors, is much more diffuse. Hence, if the scaffold binds in a mode including bridging water molecules, it has significantly more degrees of freedom to position its hydrophobic substituent optimally in the rigid pY+3 affinity pocket.

Driving Force for Inhibitor Binding. The superposition of all protein inhibitor structures indicates that there are two conserved interactions of high importance: the binding of a negatively charged group in the phosphate recognition site and the hydrophobic interaction in the pY+3 affinity pocket. The scaffolds linking these two substituents bind onto a flat surface between the two pockets.

The charged group is able to interact with R34 and R14 in two different ways. In most structures, two terminal oxygen atoms form salt bridges to both arginines. However, in some cases one terminal and one ester oxygen interact with R34, forcing the phenyl ring in a different conformation. The orientation of the phenyl ring seems to be fairly variable and to depend on additional interactions that the individual inhibitor may exhibit. The salt bridges form part of a complicated and well-conserved H-bond network connecting the individual inhibitor to the arginines and loop formed by amino acids 35–42. This network of salt bridges and H bonds is conserved in all inhibitors. It seems to be essential for the recognition of the inhibitor that the inhibitors integrate well into the H-bond network. However, since loop 35–42 can adopt a variety of different conformations, substituents that differ significantly in their size and shape are able to bind to the phosphate recognition site.²¹

The second important group is the hydrophobic substituent that points into the hydrophobic pY+3 affinity pocket formed by V96, I73, T74, and Y89. Some inhibitors, such as compounds **2–4**, reach fairly deep in the pocket, while other inhibitors, such as compound **5** and **7**, are not able to penetrate very deeply into the pocket. In these cases, there is a water molecule occupying the space between the inhibitor and the surface of the pY+3 affinity pocket. The superposition of all complex structures shows that the pY+3 pocket is very rigid with rms deviations between individual structures within the experimental error. This suggests that the shape and the size of the substituent are essential features for high-affinity inhibitor binding and only limited deviations from the ideal shape are tolerated by the protein as shown by calorimetric investigation of peptide binding and SAR data.^{16,22,25}

Driving Force for the Choice of the Inhibitor Binding Mode. All inhibitors seem to aim at filling the pY+3 pocket as much as possible and achieve that by a different interaction of the inhibitor scaffold with the protein. Inhibitors with a shortened scaffold such as compound **4** take, when possible, a shortcut on the surface of the protein compared to the natural peptide, while inhibitors such as compound **2** bind in the modus of the natural peptide. However, there are some restrictions as to which binding modus can be assumed by an individual inhibitor. These restrictions are revealed by direct structure comparisons of individual inhibitors and may help to identify the driving force for the choice of the inhibitor binding mode.

Compounds **2** and **3** differ only in their substituents in the pY+3 position. While in compound **2** there is a biphenyl group in this position, in compound **3** there is a much shorter phenylpropyl group present. However, a comparison of the two X-ray structures shows that in both structures the hydrophobic substituents penetrate similarly deeply in the hydrophobic pocket with the phenethyl group taking the place of the terminal phenyl ring of compound **2** (Figure 5a). Compound **3** achieves that by adopting a different conformation of the phenyl phosphate group.

Compounds **1** and **5** differ again only in their substituents pointing into the pY+3 position. In addition, they differ from the previous pair (compounds **2** and **3**) in that the phosphate group is replaced by an α,α -difluorobenzyl phosphonate group. A comparison of their X-ray structures (Figure 5b) shows that both compounds bind in the same mode to the SH2 domain even though the cyclohexyl group in compound **5** is too small to be positioned comfortably in the hydrophobic pocket. In contrast to the phosphotyrosine ring in compound **3**, the phosphonate moiety in compound **1** is unable to assume the alternative conformation because of steric hindrance of the fluorine atoms. Thus, the conformation adopted by compound **3** is not accessible for compound **1** and the hydrophobic interactions within the pY+3 pocket are limited, giving rise to a compound less active than **1**.

The main difference between compounds **4** and **7** is again in the substituent pointing into the pY+3 pocket. As described above, compound **4** adopts a shortcut binding mode that buries the aromatic ring deeply into the pY+3 pocket. The superposition of the two X-ray structures (Figure 5c) shows that compound **7** binds in a different binding mode, namely, that of compound **2**. However, since the acetamidomethylene insertion is missing in scaffold II, there is no interaction with H60N. A closer analysis of the complex structure with compound **7** revealed that the terminal tertiary butyl group is too bulky to slide deeper into the pocket, which puts the scaffold in a position favoring the compound **2** binding mode. A well-defined water molecule occupies the depth of the pY+3 pocket. However, the superposition of the X-ray structures of compound **7** and the pYEE1 peptide (Figure 5d) shows that in both structures the water molecule that is conserved in binding modes 1 and 2 is present and that the tertiary butyl group and the isoleucine side chain superimpose very well. Even though the scaffold of compound **7** differs substantially from the peptide backbone, the similar shape and size of the substituent in pY+3 position have induced a scaffold binding mode involving the conserved water molecule.

If the shape and size of the substituents in the pY+3 position have a strong influence on the binding mode, inhibitors with the same pY+3 substituent should assume the same binding mode. Thus, in contrast to the examples mentioned above, compounds **1**, **2**, and **8–11** have identical scaffold and pY+3 substituents but differ in the substituent pointing into the phosphate recognition site. The structure comparisons show that all these inhibitors display indeed the same binding mode and that they differ only in the binding of the phosphotyrosine replacements (Figure 6a). The IC₅₀ values of these inhibitors range from 0.25 nM for compound **10**

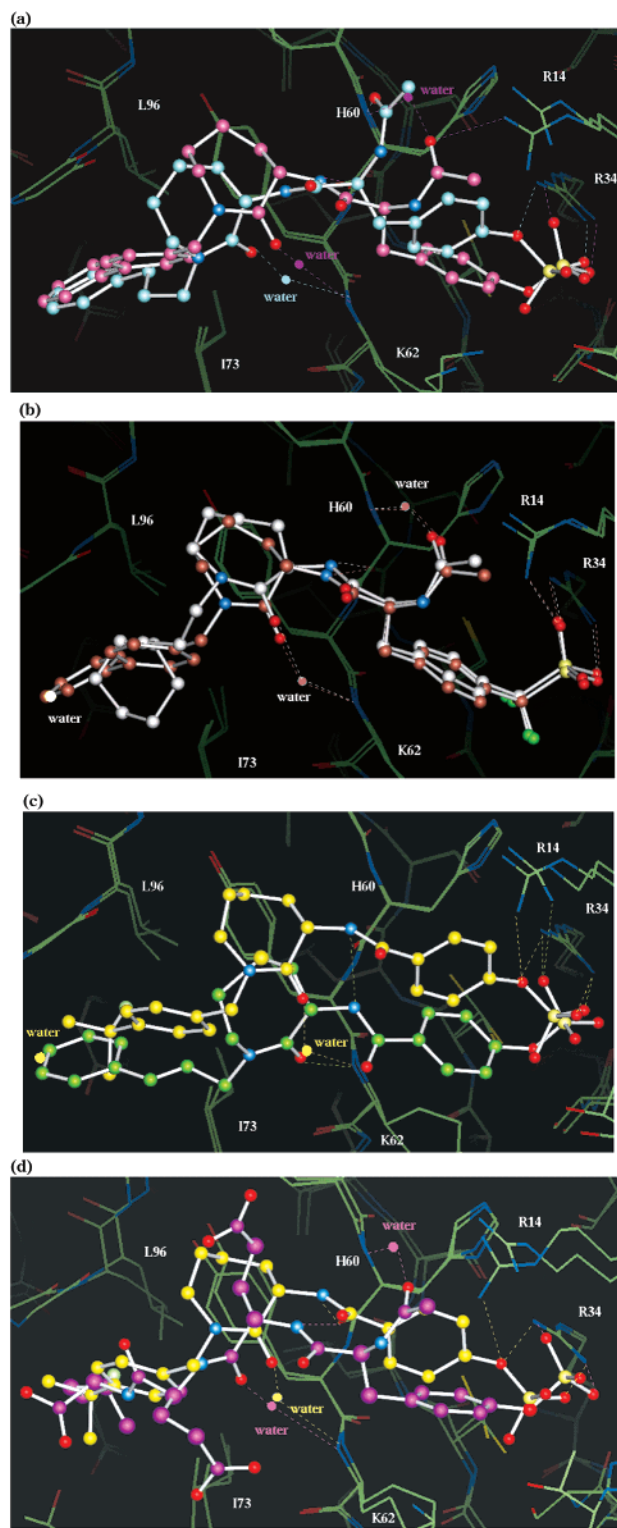


Figure 5. (a) Superposition of compounds **2** (pink) and **3** (blue) bound to the SH2 domain of src. (b) Superposition of compounds **1** (brown) and **5** (white) bound to the SH2 domain of src. (c) Superposition of compounds **4** (green) and **7** (yellow) bound to the SH2 domain of src. (d) Superposition of compounds **7** (yellow) and pYEEI²⁴ peptide (1shd, purple) bound to the SH2 domain of src.

to 2 μ M for compound **11**, reflecting the importance of the substituent pointing into the phosphotyrosine pocket.²⁶ In high-affinity inhibitors such as compound **8**, the polar headgroup integrates well in the H-bond network, but in weakly binding inhibitors such as

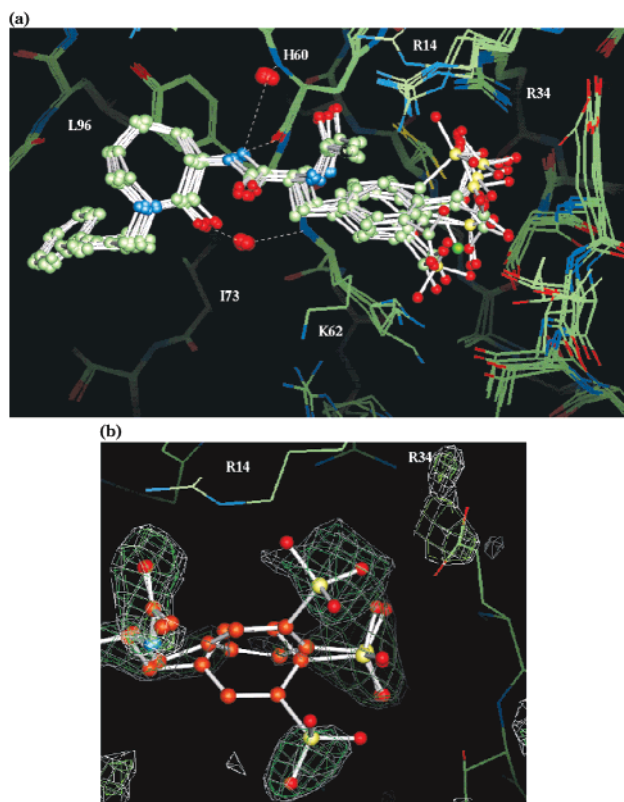


Figure 6. (a) Superposition of compounds **1**, **2**, and **8–11** bound to the SH2 domain of src. (b) Omit map of compound **11** bound to the SH2 domain of src contoured at 3σ (green) and 2.5σ (white).

compound **9**, the phosphotyrosine replacements do not fit well in the H-bond network.²¹ In particular, the bisphosphonate group in compound **11** does not integrate well into the H-bond network, which is reflected in the considerable disordered electron density of this group in the X-ray structure (Figure 6b) and the high IC_{50} value. However, even though some of these groups do not represent a good phosphotyrosine replacement, the same binding mode is maintained in all structures with a biphenyl substituent in the pY+3 position.

Discussion

The inhibitors shown here can be described as two closely related scaffolds with two substituents. The substituent pointing into the phosphotyrosine pocket consists in all cases of polar and negatively charged groups and contributes to the recognition of the inhibitor by forming an intricate H-bond network with the protein. Because of the flexibility of the phosphate recognition loop 36–42,^{8,27} the relative positions of the functional groups within the inhibitor are of minor importance and significantly different substituents are tolerated in the phosphotyrosine pocket.²¹ Also different binding modes of substituents are tolerated. In particular, there are two different modes accessible to phenyl phosphate. The second substituent points into the hydrophobic pY+3 pocket and contributes strongly to the binding affinity by its hydrophobic interactions. The superposition of all X-ray structures shows that the pY+3 pocket is unable to change its shape upon inhibitor binding, and hence, only a limited number of chemical groups fit tightly into the pocket.

The X-ray structures show that the two closely related scaffolds described here can bind in three different binding modes. The comparisons of complex structures with inhibitors differing only in their pY+3 substituents indicate that the size and shape of these substituents seem to have a strong influence on whether the inhibitor is bound in a scaffold binding mode including or excluding water molecules. If no bridging water molecule is present, the substituent has to point at the correct angle into the pocket and has to fit exactly into the hydrophobic pocket. This scaffold binding mode has been found only once in the X-ray structures, indicating that the requirements for substituents in this binding mode are very stringent. Bridging water molecules between the protein and our scaffolds increase the degree of freedom for the scaffold to position a particular hydrophobic substituent deeply in the hydrophobic pocket, and hence, a somewhat greater variety of hydrophobic substituents are tolerated. An alternative approach for the inhibitor to maximize the interaction with the hydrophobic pocket is to assume different binding modes of the phenyl phosphate in the phosphotyrosine pocket. Shorter inhibitors can stretch themselves and reach deeper into the pY+3 pocket when the phosphate binds with one terminal and one bridging water oxygen. If the pY+3 substituent is too small, an additional water molecule fills the space between the inhibitor and the pY+3 pocket.^{27,28} The data also show that flat aromatic rings such as benzyl and biphenyl rings fit much deeper in the pocket than bulky groups such as a tertiary butyl group. In summary, the X-ray structures suggest that the shape and size of the substituent pointing into the pY+3 pocket induce the binding mode in which the maximum of hydrophobic interaction between the substituent and the pY+3 pocket is achieved.

Our results show that when optimizing a substituent for a given scaffold, one should keep in mind that there might be different binding modes and that it is advisable to base the lead optimization on as many X-ray structures as possible. Could we have expected the different binding modes? Considering the flat surface with which the scaffold interacts, it becomes clear that the three main-chain atoms (H60N, H60O, and K62N) to which the scaffold has to form H bonds belong to a very rigid part of the protein. Thus, if no water molecules are included, the distances between the corresponding H-bond partners in the scaffold pharmacophore and the angle at which the substituent points into the rigid pY+3 pocket have to be within narrow limits, reducing strongly the number of scaffold candidates and substituents. When the same scaffold is used, the angular restraints for the pY+3 substituent are made less stringent by including water molecules, thereby increasing the variety of substituents that can be placed by the scaffold into the hydrophobic pocket. Including water molecules should also increase the number of putative scaffolds because the distances of the H-bond partners within these scaffolds need to be less well defined. In summary, our results suggest that the combination of a rigid scaffold binding surface to which the scaffold forms H bonds and the rigid pY+3 pocket has given rise to binding modes in which water molecules compensate for the restraints. With hindsight of the first X-ray structures, this might have been expected.

The importance of the two water molecules is confirmed by other crystal structures of SH2 domains. Crystals structures have been described from a variety of different SH2 domains including the SH2 domains of pp60src kinase^{9,29,30}, p56lck kinase,^{27,28} and Grb2 adaptor protein.^{11,12} In the structure of the KPFpYYVNV peptide complexed to the SH2 domain of GRRB2, the peptide is bound in a β -turn conformation without mediating water molecules.¹¹ However, most peptide and peptide-related inhibitors bind to the corresponding SH2 domain in an extended conformation involving interaction between main-chain atoms of the protein and the peptide such as the highly conserved H bond between the amide of the pY+1 residue and the peptide carbonyl of H60 or equivalent residue in other SH2 domains. The structures also include two highly conserved water molecules bridging backbone atoms of the peptide inhibitor and SH2. Even in structures with bound low-affinity peptides,³¹ these two water molecules are located at the same position and correspond to the water molecules that were found to mediate the interaction of our scaffolds with the SH2 domain of pp60src.

Water molecules mediating the binding of inhibitors to the protein are considered, for entropical reasons, less favorable and were successfully replaced by inhibitor atoms in projects such as the HIV-1 protease.³² Inhibitors of SH2 domains with non-peptidic scaffolds have been described, and in some compound classes, water molecules were present, mediating the interaction between the non-peptidic inhibitor and the SH2 domain.^{10,30} Lunney et al. (1997) have designed non-peptidic pp60src SH2 inhibitors based on a peptide structure with the aim to replace bridging water molecules with inhibitor atoms. The crystallographic structure of a compound with a dimethylphenyl moiety as the pY+3 substituent showed that indeed the water molecule that binds in the peptide structure to K62N has been replaced by an H-bond acceptor from the inhibitor scaffold. However, very much to their surprise, the phosphotyrosine group binds in a novel conformation and the dimethylphenyl moiety points deeper in the pY+3 pocket. Considering their figures, it seems that the phenyl phosphate is in a conformation similar to the one that has been described above for the binding of compound **3** and that the dimethylphenyl moiety may very well superimpose with the terminal aromatic group of compound **3**. Similar to what has been described above, the phenyl phosphate in compound **5** of Lunney et al.⁹ assumes a conformation that enables the inhibitor to bury the flat dimethylphenyl moiety deep in the pY+3 pocket. Other complexes in which the shape and size of the inhibitor substituent pointing in the pY+3 pocket seem to have induced the alternative conformation of the phenyl phosphate includes complex **5**.²⁹ The superposition of the corresponding X-ray structure with the structure of compound **3** shows that the phosphotyrosine is present in the same binding mode and that the cyclohexyl group of compound **5**²⁹ indeed is positioned as deeply in the pY+3 pocket as the substituent in compound **3**. A similar binding mode of the phosphotyrosine had been described before only for the SH2 domain of Syp in which a glycine is present at the equivalent position of R14.³¹

These results suggest that the inhibitors bind in a mode that maximizes the hydrophobic interaction in the pY+3 pocket. This is achieved by including water molecules and/or a change in the conformation of the substituent pointing into the phosphotyrosine pocket. As found in other cases,^{33,34} the water molecules form an integral part of the protein–ligand interface and increase the flexibility of the interface between a rigid inhibitor part and a rigid protein surface. For structure-based drug design, it is important to know the binding modes of a given compound class and the chemical features according to which individual binding modes are assumed. However, there is not necessarily the same correlation between these chemical factors and IC₅₀ values, since for low IC₅₀ values other factors such as the number of freely rotating bonds frozen upon binding and any induced strain in the inhibitor conformation play an additional role.

Acknowledgment. The authors thank Herman Schreuder for helpful discussions and Alexander Liesum for excellent technical assistance. This work was done during the course of collaboration with ARIAD Pharmaceuticals, and we are grateful to T. Sawyer and M. Hatada for stimulating discussions.

References

- Brown, M. T.; Cooper, J. A. Regulation, substrates and functions of src. *Biochim. Biophys. Acta* **1996**, *1287*, 121–149.
- Boyce, B. F.; Yoneda, T.; Lowe, C.; Soriano, P.; Mundy, G. Requirement of pp60c-src expression for osteoclasts to form ruffled borders and resorb bone in mice. *J. Clin. Invest.* **1992**, *90*, 1622–1627.
- Soriano, P.; Montgomery, C.; Geske, R.; Bradley, A. Targeted disruption of the c-src proto-oncogene leads to osteopetrosis in mice. *Cell* **1991**, *64*, 693–702.
- Schaffhausen, B. SH2 domain structure and function. *Biochim. Biophys. Acta* **1995**, *1242*, 61–75.
- Waksman, G.; et al. Crystal structure of the phosphotyrosine recognition domain SH2 of v-src complexed with tyrosine-phosphorylated peptides. *Nature* **1992**, *358*, 646–653.
- Waksman, G.; Shoelson, S. E.; Pant, N.; Cowburn, D.; Kuriyan, J. Binding of a high affinity phosphotyrosyl peptide to the src sh2 domain: crystal structures of the complexed and peptide-free form. *Cell* **1993**, *72*, 779–790.
- Eck, M. J.; Atwell, S. K.; Shoelson, S. E.; Arrison, S. S. Structure of the regulatory domains of the src-family tyrosine kinase Lck. *Nature* **1994**, *368*, 764–769.
- Clarifson, P. S.; et al. Peptide Ligands of pp60c-src SH2 domains: a thermodynamic and structural study. *Biochemistry* **1997**, *36*, 6283–6293.
- Lunney, E. A.; et al. Structure-based design of a novel series of nonpeptide ligands that bind to the pp60src SH2 domain. *J. Am. Chem. Soc.* **1997**, *119*, 12471–12476.
- Shakespeare, W.; et al. Structure-based design of an osteoclast-selective, nonpeptide src homology 2 inhibitor with in vivo antiresorptive activity. *Proc. Natl. Acad. Sci. U.S.A.* **2000**, *97*, 9373–9378.
- Rahuel, J. Structural basis for specificity of grb2-sh2 revealed by a novel ligand binding mode. *Nat. Struct. Biol.* **1996**, *3*, 586–589.
- Rahuel, J. Structural basis for the high affinity of aminoaromatic SH2 phosphopeptide ligands. *J. Mol. Biol.* **1998**, *279*, 1013–1022.
- Mathews, I. I.; et al. Crystallographic Structures of thrombin complexed with thrombin receptor peptides: Existence of expected and novel binding modes. *Biochemistry* **1994**, *33*, 3266–3279.
- Strickland, C. L. Biochemical and crystallographic characterization of homologues non-peptidic thrombin inhibitors having alternate binding modes. *Acta Cryst.* **1998**, *D54*, 1207–1215.
- Hatada, M. H. Personal communication.
- Lesuisse, D.; Deprez, P.; Albert, E.; Duc, T. T.; Sortais, B.; Gofflo, D.; Jean-Baptiste, V.; Marquette, J.-P.; Schoot, B.; Sarubbi, E.; Lange, G.; Broto, P.; Mandine, E. Discovery of Thioazepinone Ligands for Src SH2: From Non-specific to Specific Binding. *Bioorg. Med. Chem. Lett.* **2001**, *11* (16), 2127–2131.

- (17) Kabsch, W. Automatic processing of rotation diffraction data from crystals of initially unknown symmetry and cell constants. *J. Appl. Crystallogr.* **1993**, *26*, 795–800.
- (18) Brunger, A. T.; Kurkowski, A.; Erickson, J. W. Slow-cooling protocols for crystallographic refinement by simulated annealing. *Acta Crystallogr.* **1990**, *A46*, 46–57.
- (19) Oldfield, T. J.; Hubbard, R. E. *Proteins* **1994**, *18* (4) 324–337.
- (20) Kabsch, W. A discussion of the solution for the best rotation to relate two sets of vectors. *Acta Crystallogr.* **1978**, *A34*, 827–828.
- (21) Lange, G.; Lesuisse, D.; Deprez, P.; Schoot, B.; Loenze, P.; Bénard, D.; Marquette, J.-P.; Broto, P.; Sarubbi, E.; Mandine, E. Manuscript in preparation.
- (22) Deprez, P.; Mandine, E.; Gofflo, D.; Meunier, S.; Lesuisse, D. Small ligands interacting with the phosphotyrosine binding pocket of the Src SH2 protein. *Bioorg. Med. Chem. Lett.*, in press.
- (23) Deprez, P.; Baholet, I.; Burlet, S.; Lange, G.; Ahoot, B.; Vermond, A.; Mandine, E.; Lesuisse, D. Discovery of highly potent Src SH2 binders: Structure–activity studies and x-ray structures. *Bioorg. Med. Chem. Lett.*, in press.
- (24) Gilmer, T.; Rodriguez, M.; Jordan, S.; Crosby, R.; Alligood, K.; Green, M.; Kimery, M.; Wagner, C.; Kinder, D. Peptide inhibitors of src SH3–SH2 phosphoprotein interactions. *J. Biol. Chem.* **1994**, *269*, 31711–31719.
- (25) Bradshaw, J. M.; Waksman, G. Calorimetric Examination of High Affinity src SH2 Domain-Tyrosyl Phosphopeptide Binding: Dissection of the Phosphopeptide Sequence Specificity and Coupling Energetics. *Biochemistry* **1999**, *38*, 5147–5154.
- (26) Bradshaw, J. M.; Mitaxov, V.; Waksman G. Investigation of Phosphotyrosine Recognition by the SH2 Domain of the Src Kinase. *J. Mol. Biol.* **1999**, *293*, 971–985.
- (27) Mikol, V.; Baumann, G.; Keller, T. H.; Manning, U.; Zurini, M. G. M. The crystal structures of the SH2 domain of p56lck complexed with two phosphopeptides suggest a gated peptide binding site. *J. Mol. Biol.* **1995**, *246*, 344–355.
- (28) Tong, L.; Warren, T. C.; King, J.; Betageri, R.; Rose, J.; Jakes, S. Crystal structures of the human p56lck SH2 domain in complex with two short phosphotyrosyl peptides at 1.0 Å and 1.8 Å. *J. Mol. Biol.* **1996**, *256* 601–610.
- (29) Plummer, M. S.; et al. Design, synthesis, and cocrystal structure of a non-peptide src SH2 domain ligand. *J. Med. Chem.* **1997**, *40*, 3719–3725.
- (30) Buchanan, J. L.; et al. Structure-based design and synthesis of a novel class of src SH2 inhibitors. *Bioorg. Med. Chem. Lett.* **1999**, *9*, 2353–2358.
- (31) Lee, Ch.-H.; Kominos, D.; Jacques, S.; Margolis, B.; Schlessinger, J.; Shoelson, S. E.; Juriyan, J. Crystal structures of peptide complexes of the amino-terminal SH2 domain of the Syp tyrosine phosphatase. *Structure* **1994**, *2*, 423–438.
- (32) Lam, P. Y. S.; et al. Rational design of potent, bioavailable, nonpeptidic cyclic ureas as HIV protease inhibitors. *Science* **1994**, *263*, 380–384.
- (33) Minke, W. E.; Diller, D. J.; Hol, W. G.; Verlinde, C. L. The role of waters in docking strategies with incremental flexibility for carbohydrate derivatives: heat-labile enterotoxin, a multivalent test case. *J. Med. Chem.* **1999**, *42*, 1778–1788.
- (34) Rarey, M.; Kramer, B.; Lengauer, T. The particle concept: placing water molecules during protein–ligand docking predictions. *Proteins: Struct., Funct., Genet.* **1999**, *34*, 17–28.

JM0110800